Mode identification from time series of high-resolution high signal-to-noise spectroscopy

1. Aerts et al. (1992), Briquet & Aerts (2003)
2. Telting & Schrijvers (1997)
3. Zima (2006, 2008): FAMIAS

Example: 12 Lacertae (Mathias et al. 2004)

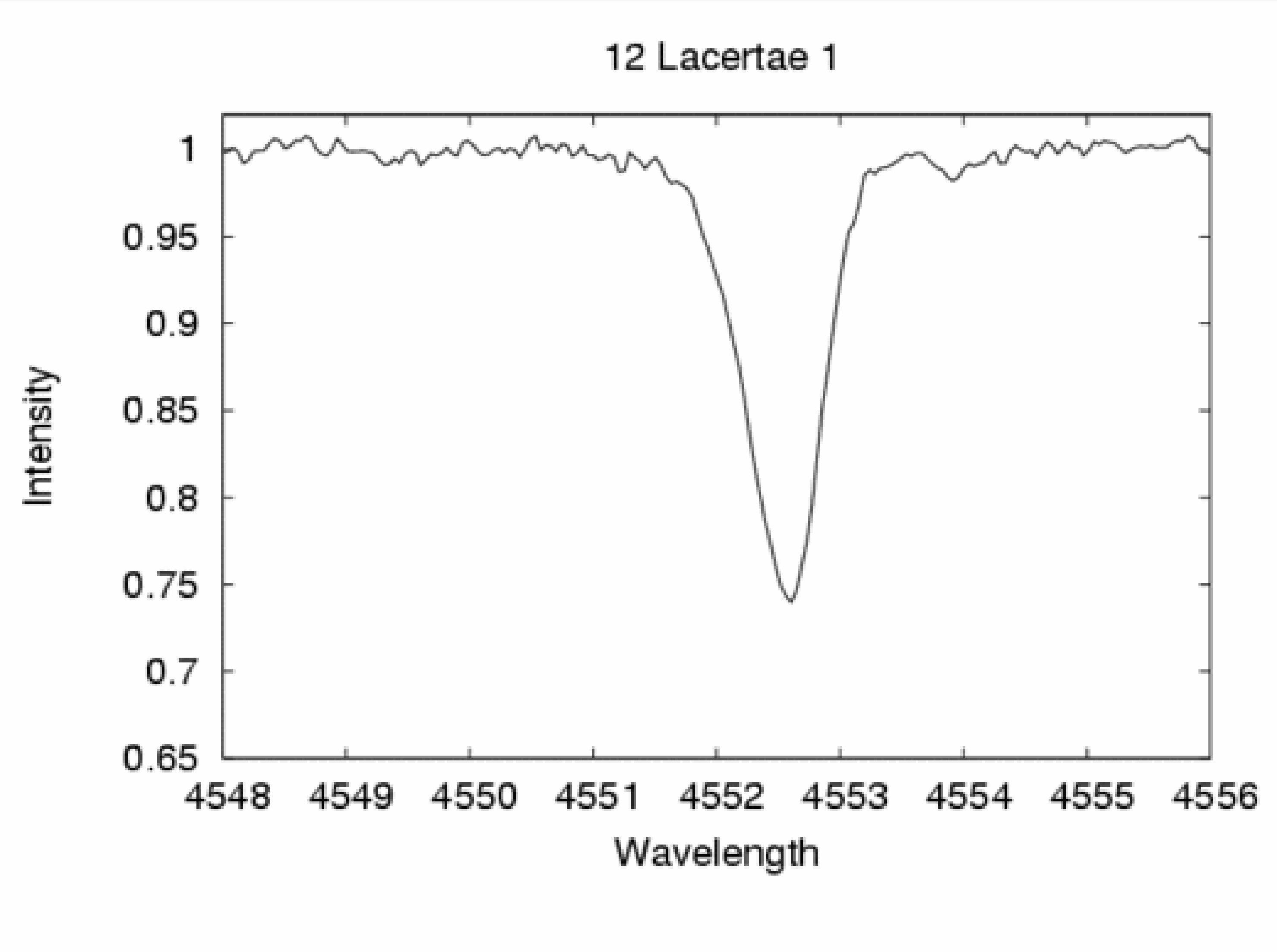

Example: Rho Puppis (Mathias et al. 1997)

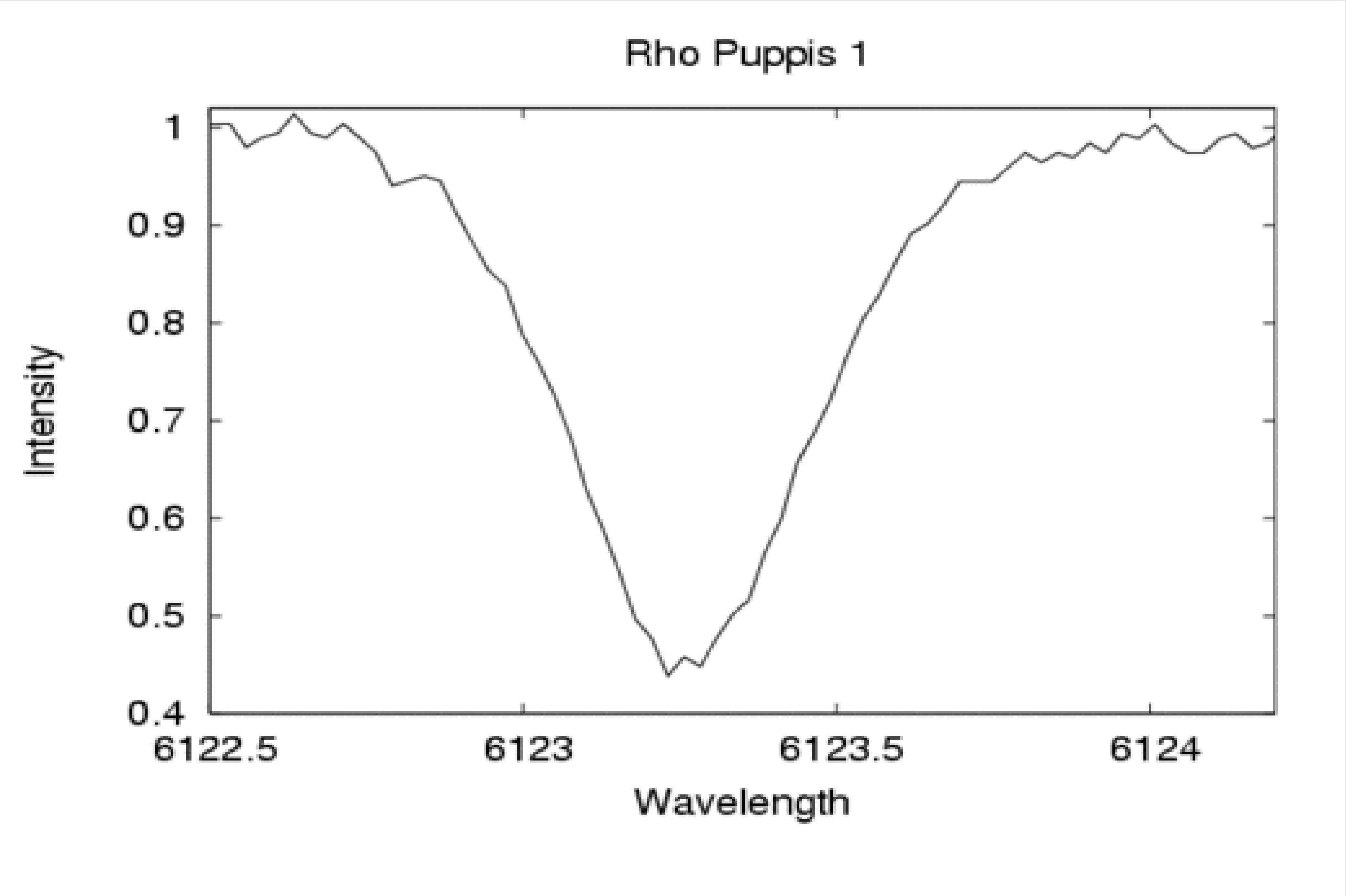

Mode identification from LPVs

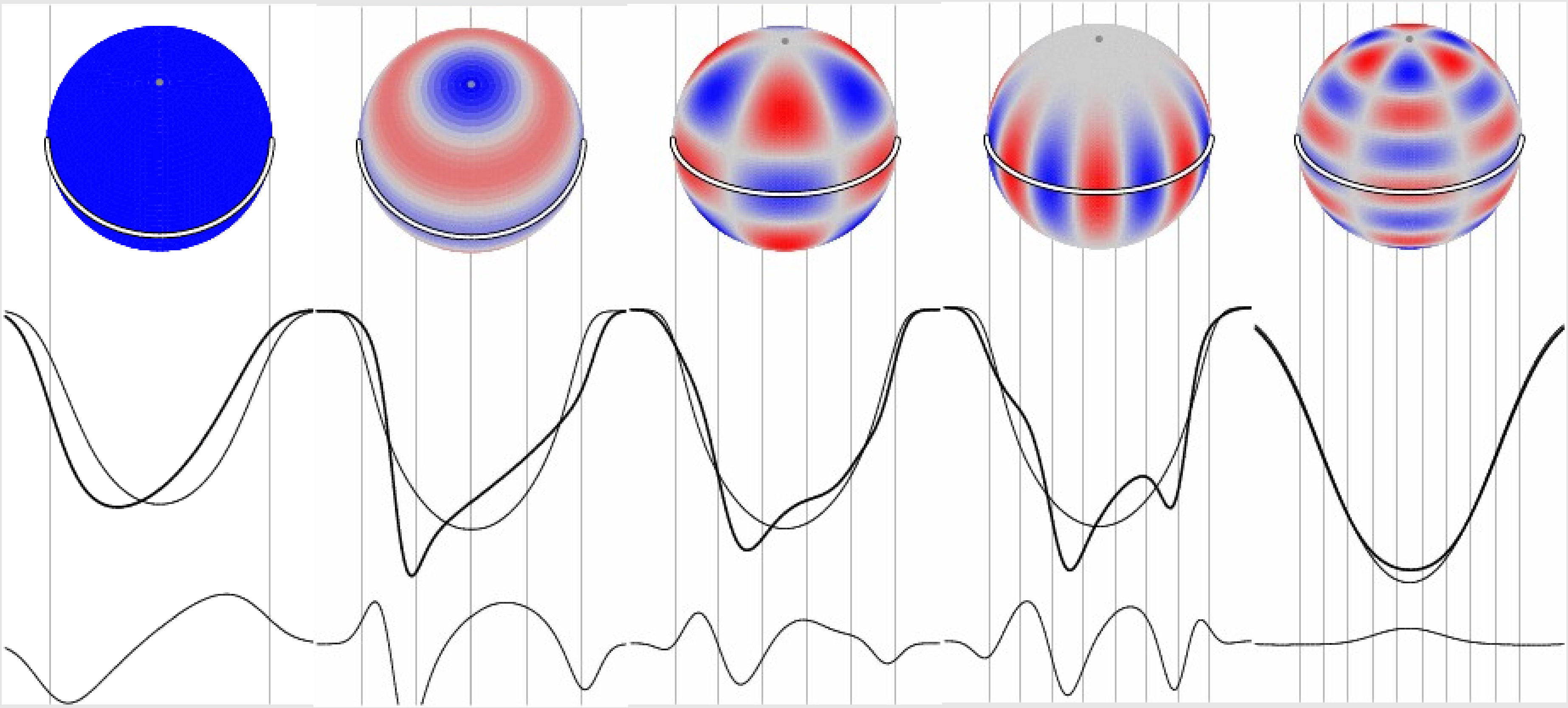

Animations from John Telting and Coen Schrijvers

Analysis of line-profile variations

- Goal: derive empirical mode identification as input for asteroseismic modelling
- Use several diagnostics: moments of the line; amplitude and phase across spectral line
- Calibrate methods from extensive simulations + theory of non-radial oscillations

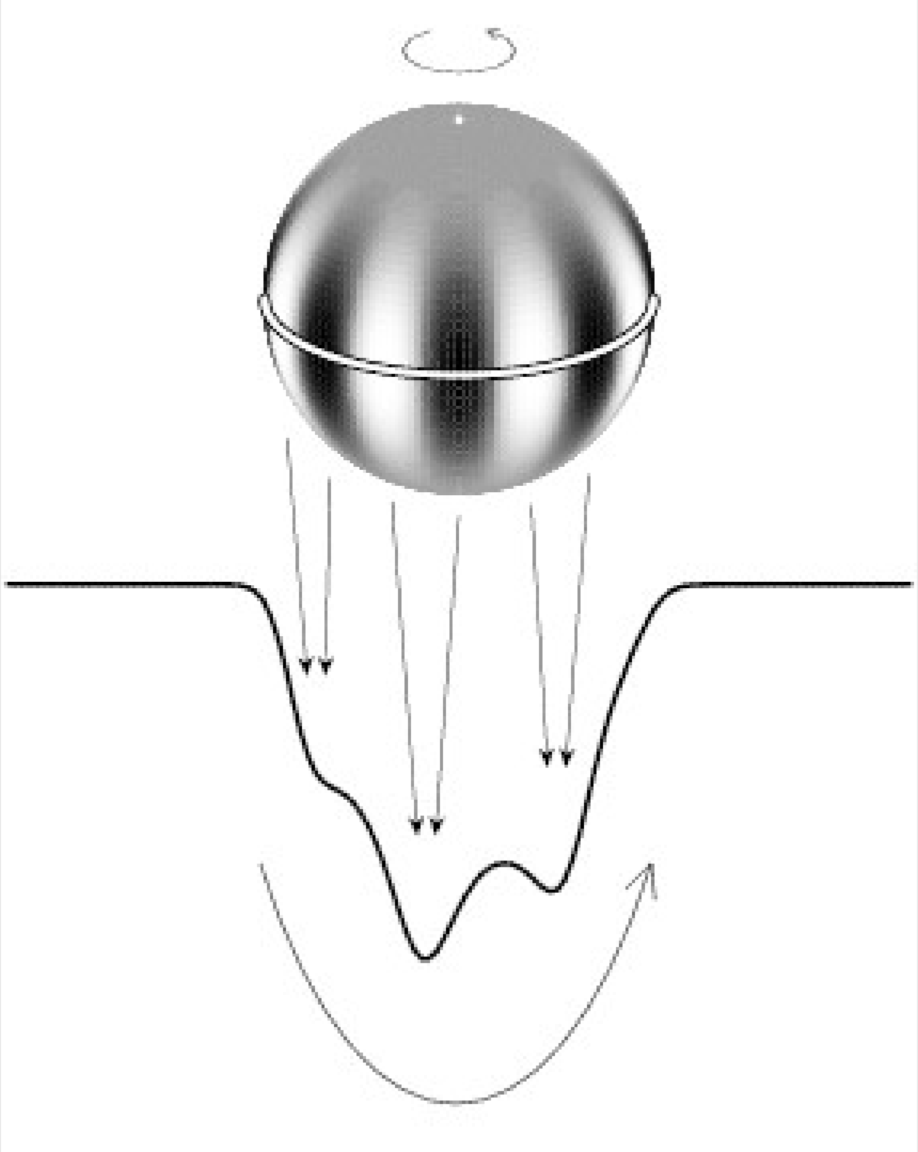

Requirements for mode identification

- Use non-blended lines or averages thereof or cross-correlation profiles
- Cover entire beat cycle of all modes
- S/N > 300
- R > 50 000
- # > several hundred (say 100 per mode)

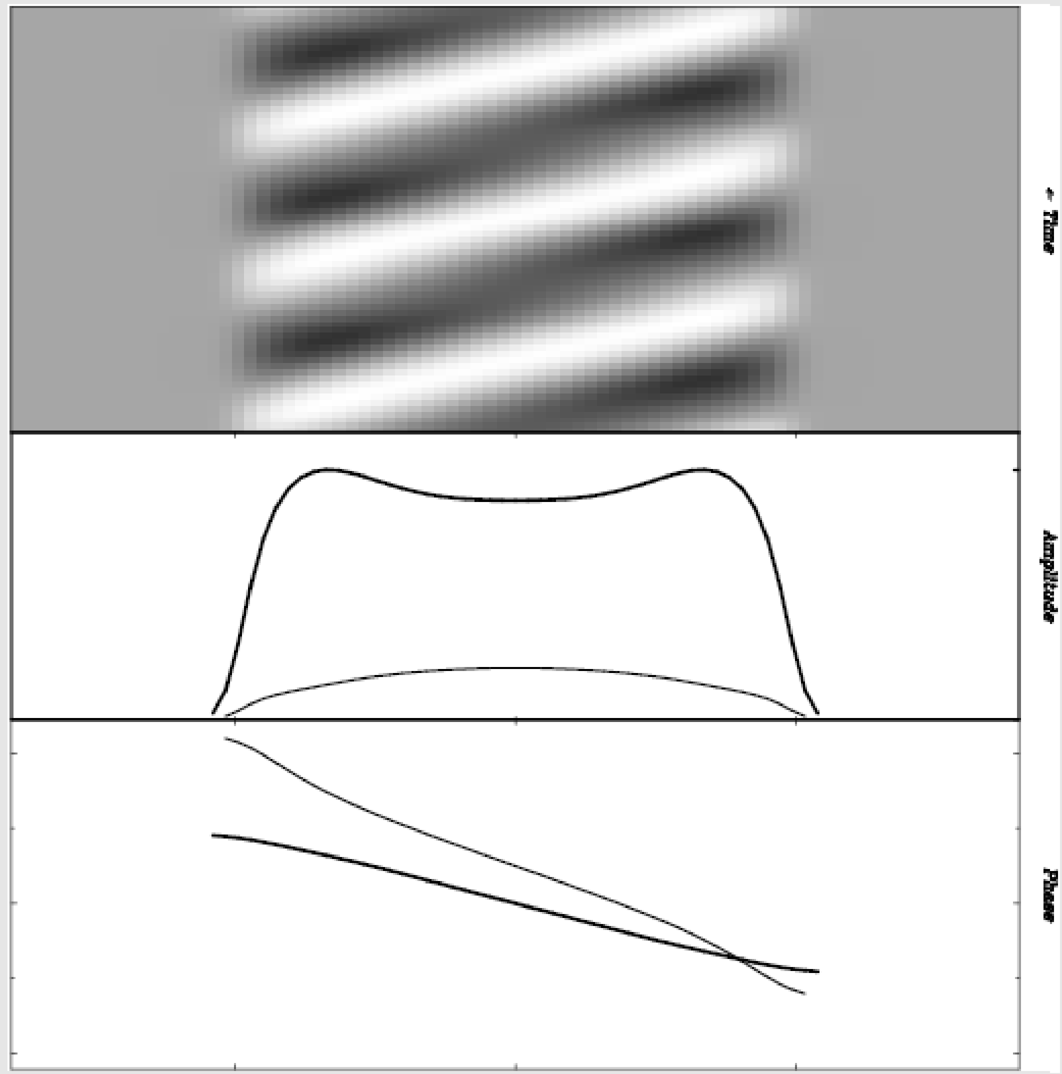

Different line broadening mechanisms

1. *Atomic broadening* caused by finite lifetime of energy levels of ions: **Lorentz profile**

2. *Pressure broadening* due to neighbouring particles disturbing energy levels of ions, causing a small change in the wavelength of the spectral line: **Lorentz profile**

3. *Thermal broadening* due to Maxwellian velocity law with a temperature dependence $\sim \sqrt{T}$: **Gaussian profile**

4. *Rotational broadening*, assumed to be uniform across the stellar disk, and time independent: $v(R, \theta, \phi) = -\Omega R \sin i \sin \theta \sin \phi$

5. *Pulsational broadening*: profile shape determined by the parameters occurring in the expression of the pulsation velocity, including (l, m) of all the oscillation modes

1,2,3 follow from atmosphere models, but too uncertain in practice.... we take them together in intrinsic profile and fit

Theoretical computation of LPVs

- <u>Assumptions :</u>

  spherically symmetric equilibrium i.e.

  - slow rotation ($\Omega/\omega \leq 1$)
  - velocities $<<$ break-up

  no magnetic field

- A rotating, pulsating star : $\vec{v} = \vec{v}_{\text{rot}} + \vec{v}_{\text{puls}}$ with

$$\vec{v}_{\text{puls}} = N_\ell^m v_{\text{p}} \left(1, K\frac{\partial}{\partial\theta}, \frac{K}{\sin\theta}\frac{\partial}{\partial\varphi}\right) Y_\ell^m(\theta,\varphi) \exp(\mathrm{i}\omega t)$$

- Observations of a real rotating pulsating star :
  $\vec{v} = \vec{v}_{\text{rot}} + \vec{v}_{\text{puls}}$ convolved with an intrinsic profile, often assumed to be Gaussian $N(0, \sigma^2)$

NOT restricted to Gaussian, but atmosphere model needs to be adapted to the data itself...

Theoretical computation of LPVs

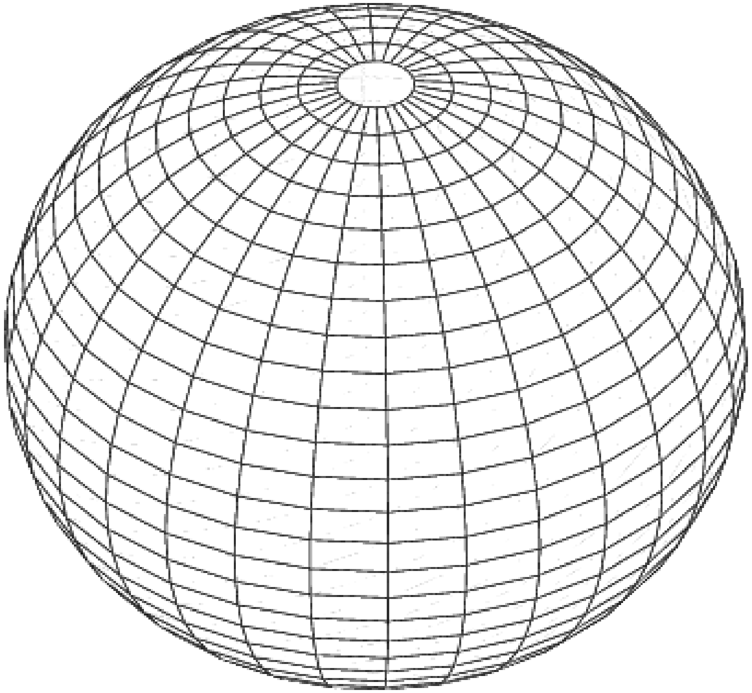

Divide stellar surface into large number of segments, typically > 5000

Compute for each segment: pulsation and rotation velocity, intensity

Project onto the line-of-sight

Add up all contributions

Theoretical computation of LPVs

1. $h_\lambda(\theta) = 1 - u_\lambda + u_\lambda \cos\theta$

2. for each point $P(R,\theta,\varphi)$:

   $$I_\lambda(\theta,\varphi)R^2 \sin\theta \; d\theta \; d\varphi = I_0 h_\lambda(\theta) R^2 \sin\theta \cos\theta \; d\theta \; d\varphi$$

3. $$\frac{\lambda_{ij} - \lambda_0}{\lambda_0} = \frac{\lambda(\theta_i,\varphi_j) - \lambda_0}{\lambda_0} = \frac{\triangle\lambda(\theta_i,\varphi_j)}{\lambda_0} = \frac{v(\theta_i,\varphi_j)}{c}$$

4. $$p(\lambda) = \sum_{i,j} \frac{I(\theta_i,\varphi_j)}{\sqrt{2\pi}\sigma} \exp\left(-\frac{(\lambda_{ij}-\lambda)^2}{2\sigma^2}\right) R^2 \sin\theta_i \triangle\theta_i \triangle\varphi_j$$

Generalisations :

a. inclusion of Coriolis correction terms

b. inclusion of temperature effects: EW variations & intensity variations

c. intrinsic profile: Voigt, based on atmosphere model

d. variable surface size and normal

Theoretical computation of LPVs

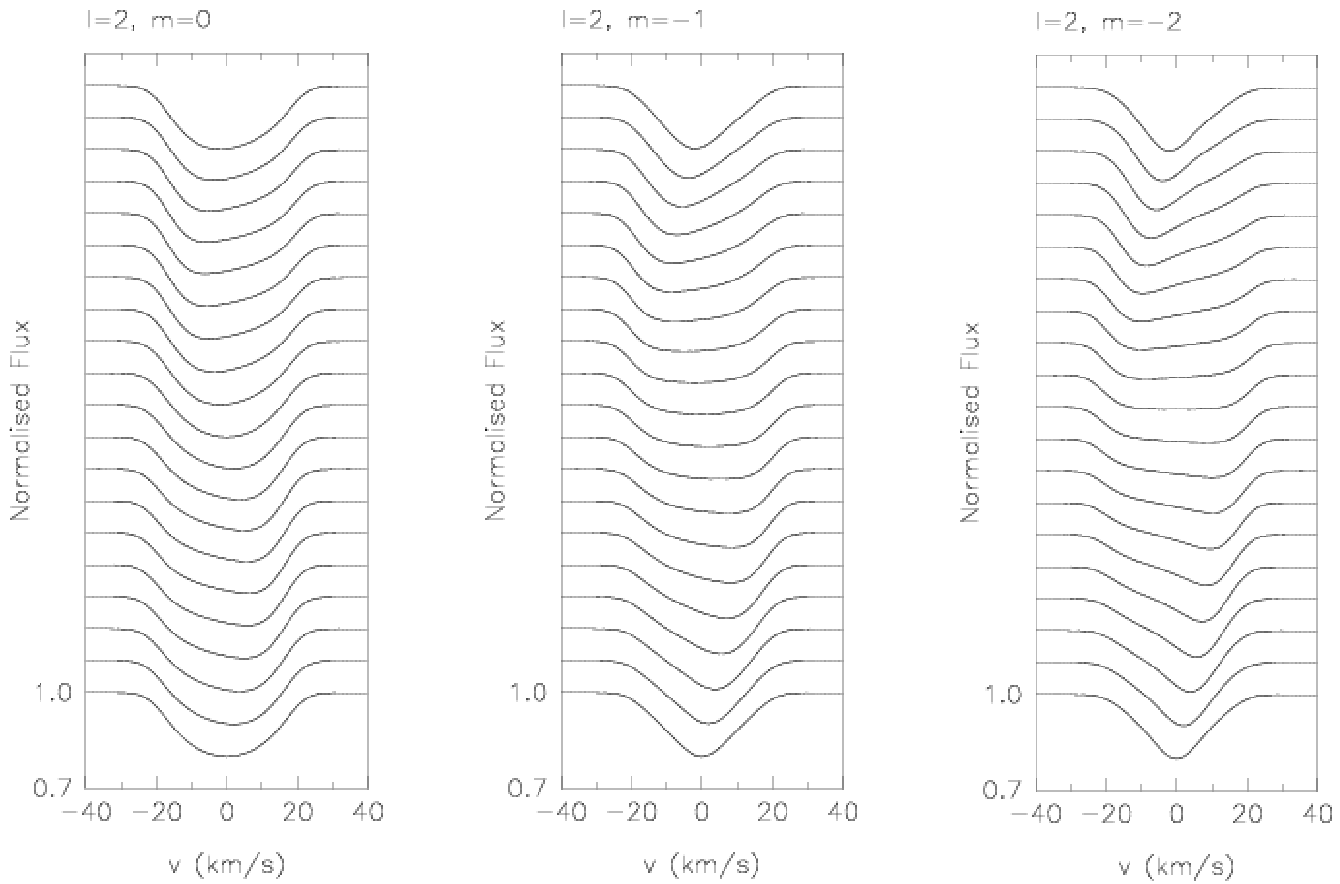

Theoretical computation of LPVs

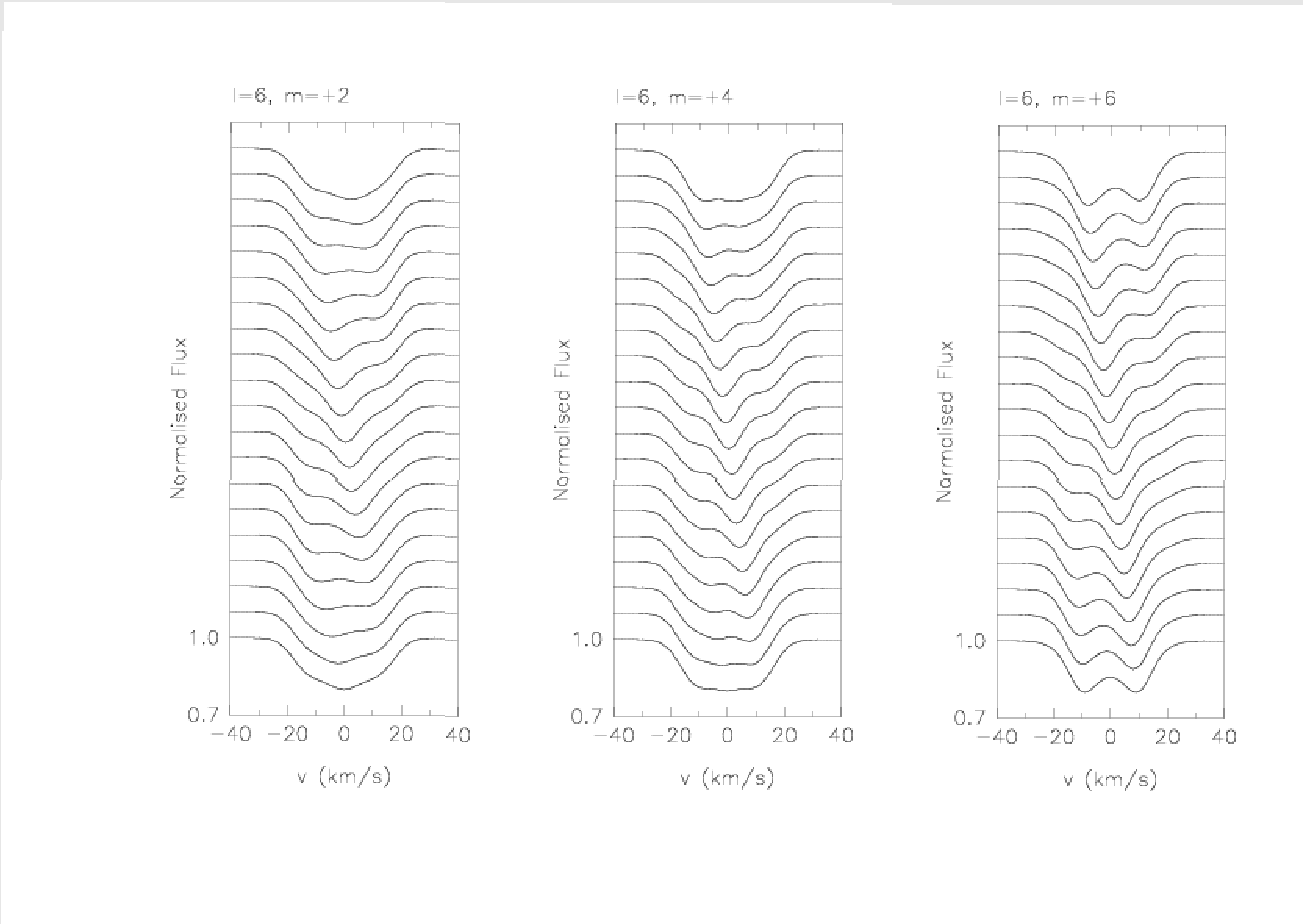

The moment method

Only applicable to slow rotators (in sense: Prot $>>$ Ppuls) !

Definition

$$< v^n >_{f*g} \equiv \frac{\int_{-\infty}^{+\infty} v^n f(v) * g(v)\, dv}{\int_{-\infty}^{+\infty} f(v) * g(v)\, dv}$$

v from pulsation eigenfunction & rotation in line-of-sight

$f(v)$ contains limb-darkening and surface-element size

$g(v)$ is due to thermal broadening (Gaussian profile)

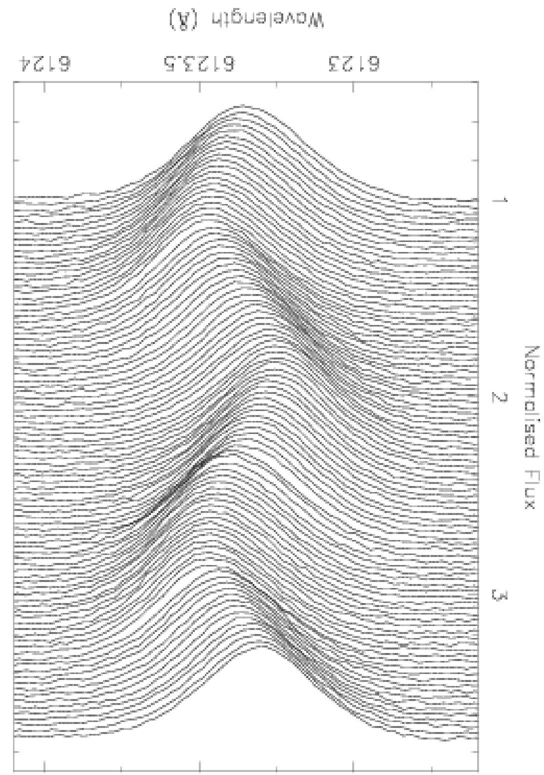

Moments of Delta Sct star Rho Puppis

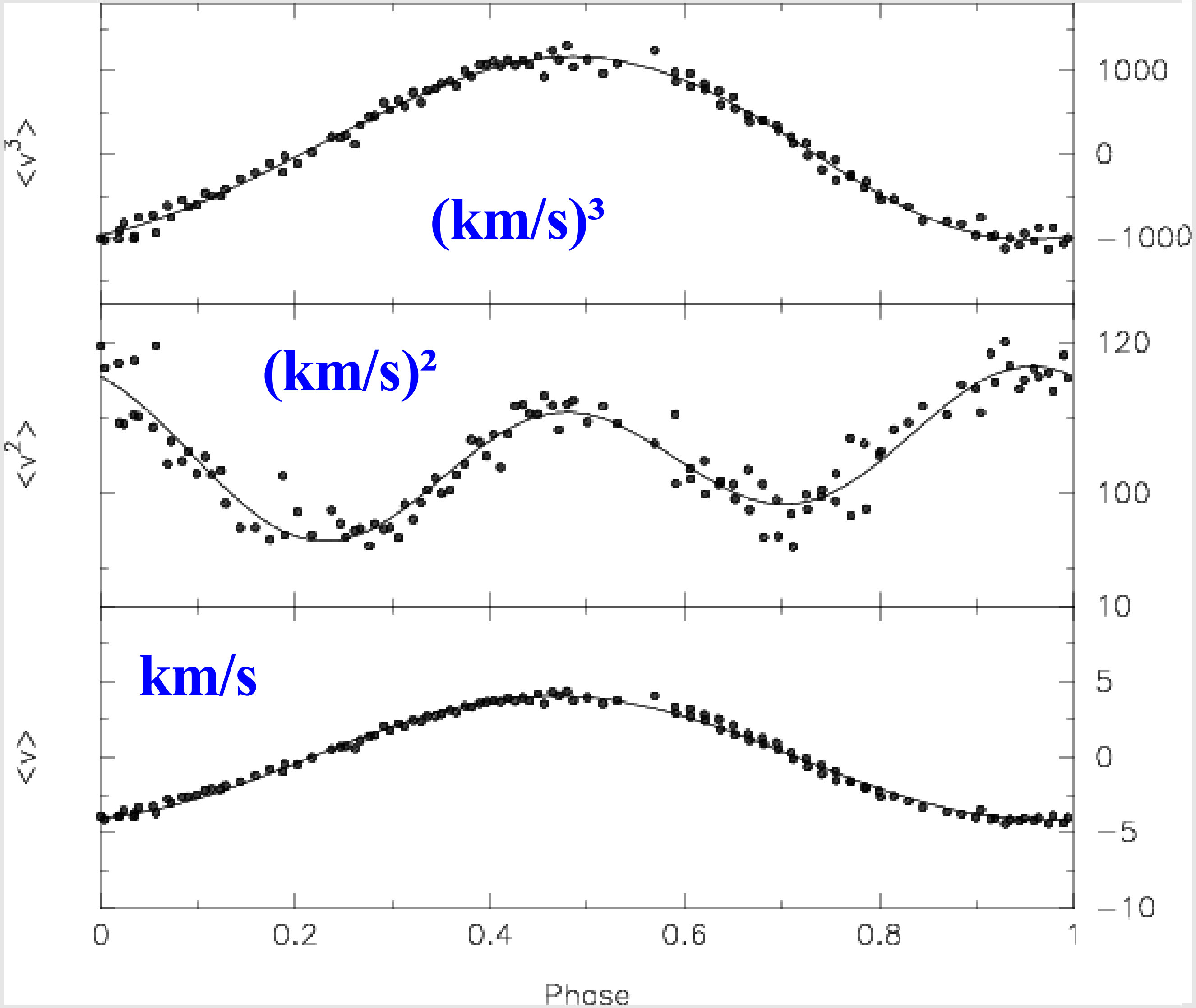

first moment: sinusoidal (ideal for frequency determination)

second moment: double sine is dominant over sine (m=0)

third moment: sine is dominant, but contributions from 2f and 3f

Note: odd moments have average = 0

Theoretical moment expressions

$$< v >_{f*g} = v_{\rm p} A(\ell, m, i) \sin(\omega t + \psi),$$

$$\begin{aligned} < v^2 >_{f*g} = & \, v_{\rm p}^2 C(\ell, m, i) \sin(2\omega t + 2\psi + \tfrac{3\pi}{2}) \\ & + v_{\rm p} v_{\Omega} D(\ell, m, i) \sin(\omega t + \psi + \tfrac{3\pi}{2}) \\ & + v_{\rm p}^2 E(\ell, m, i) + \sigma^2 + b_2 v_{\Omega}^2, \end{aligned}$$

$$\begin{aligned} < v^3 >_{f*g} = & \, v_{\rm p}^3 F(\ell, m, i) \sin(3\omega t + 3\psi) \\ & + v_{\rm p}^2 v_{\Omega} G(\ell, m, i) \sin(2\omega t + 2\psi + \tfrac{3\pi}{2}) \\ & + \left[v_{\rm p}^3 R(\ell, m, i) + v_{\rm p} v_{\Omega}^2 S(\ell, m, i) + v_{\rm p} \sigma^2 T(\ell, m, i) \right] \\ & \times \sin(\omega t + \psi). \end{aligned}$$

Aerts et al. (1992), Aerts (1996)

Partial cancellation

Limb-darkening effect

$$A(l,m,i) = a_{l,m,0}(i) \cdot a(l,K,h_\lambda)$$

Geometric effect

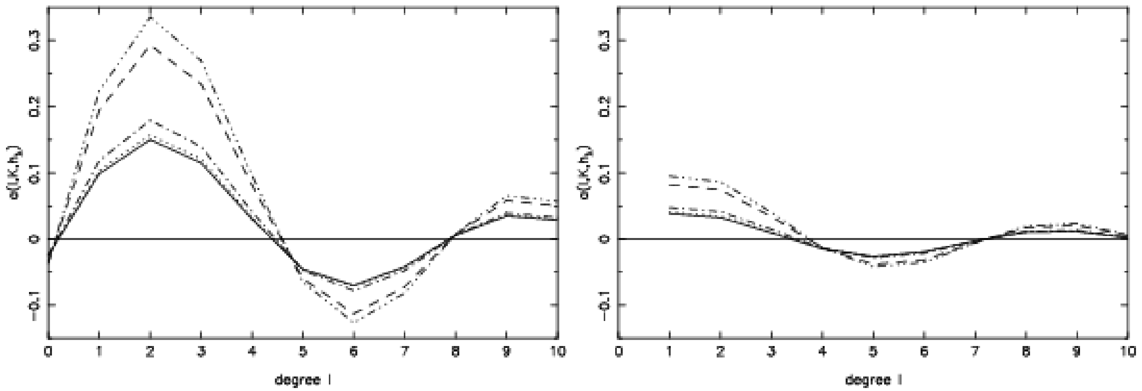

p-mode with K=0.1   g-mode with K=10.

Partial cancellation is different in spectroscopy than in photometry!

Computation of observed moments

Measurements in time series: (t_j, x_i, I_i)
j=1,...,M; i=1,...,N with N # pixels in line profile

a. Small unnormalised moments:

$$\begin{cases} m_0 = \sum_{i=1}^{N} (1 - I_i) \triangle x_i \\ m_1 = \sum_{i=1}^{N} (1 - I_i) x_i \triangle x_i \\ m_2 = \sum_{i=1}^{N} (1 - I_i) x_i^2 \triangle x_i \\ m_3 = \sum_{i=1}^{N} (1 - I_i) x_i^3 \triangle x_i \end{cases}$$

Correction of Earth motion around the Sun is taken into account, i.e. we work barycentrically

Computation of observed moments

b. Large unnormalised moments:

use $x_0 = m_1/m_0$ as a reference value:

$$\begin{cases} M_0 = \sum_{i=1}^{N} (1 - I_i) \triangle x_i \\ M_1 = \sum_{i=1}^{N} (1 - I_i)(x_i - x_0) \triangle x_i \\ M_2 = \sum_{i=1}^{N} (1 - I_i)(x_i - x_0)^2 \triangle x_i \\ M_3 = \sum_{i=1}^{N} (1 - I_i)(x_i - x_0)^3 \triangle x_i \end{cases}$$

This leads to odd moments with average zero.

c. Observed normalised moments: $< v^j >= M_j/M_0$ for $j = 1, \ldots, 3$

Dimensions are km/s, (km/s)^2 and (km/s)^3 for $j = 1, 2, 3$.

Definition of a discriminant

compare the amplitudes of theoretically calculated moments and observed moments. Definition :

$$\Gamma_\ell^m(\ v_{\rm p}, i, v_{\Omega}, \sigma) \equiv \Big[\big| AA - v_{\rm p} |A(\ell,m,i)| f_{AA} \big|^2$$
$$+ \Big(\big| CC - v_{\rm p}^2 |C(\ell,m,i)| \big|^{1/2} f_{CC} \Big)^2$$
$$+ \Big(\big| DD - v_{\rm p} v_{\Omega} |D(\ell,m,i)| \big|^{1/2} f_{DD} \Big)^2$$
$$+ \Big(\big| EE - v_{\rm p}^2 |E(\ell,m,i)| - \sigma^2 - b_2 v_{\Omega}^2 \big|^{1/2} f_{EE} \Big)^2$$
$$+ \Big(\big| FF - v_{\rm p}^3 |F(\ell,m,i)| \big|^{1/3} f_{FF} \Big)^2$$
$$+ \Big(\big| GG - v_{\rm p}^2 v_{\Omega} |G(\ell,m,i)| \big|^{1/3} f_{GG} \Big)^2$$
$$+ \Big(\big| RST - v_{\rm p}^3 |R(\ell,m,i)| - v_{\rm p} v_{\Omega}^2 |S(\ell,m,i)|$$
$$- v_{\rm p} \sigma^2 |T(\ell,m,i)| \big|^{1/3} f_{RST} \Big)^2 \Big]^{1/2}.$$

(Aerts, 1996)

Gain in data quality from 1980 - 1995

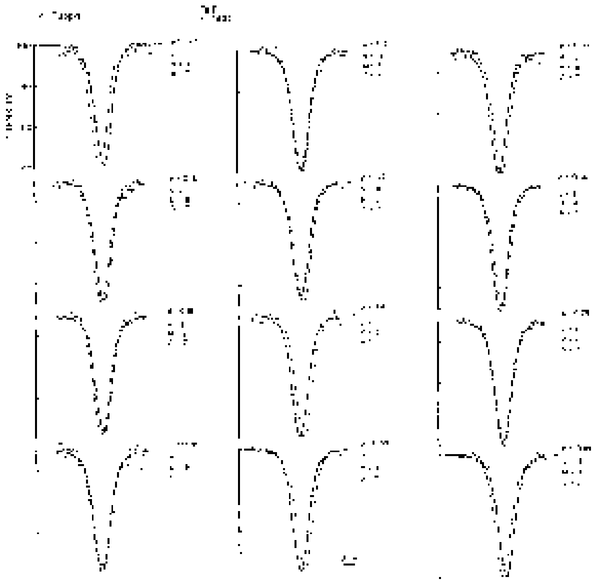

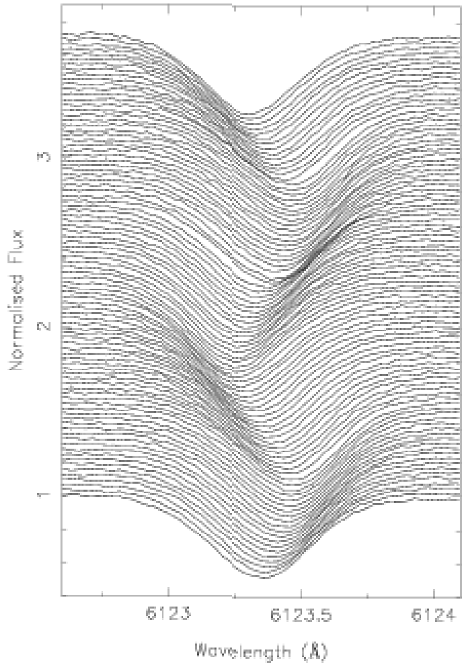

Smith et al. (1980) versus Mathias et al. (1997)

Moment method: Briquet & Aerts (2003)

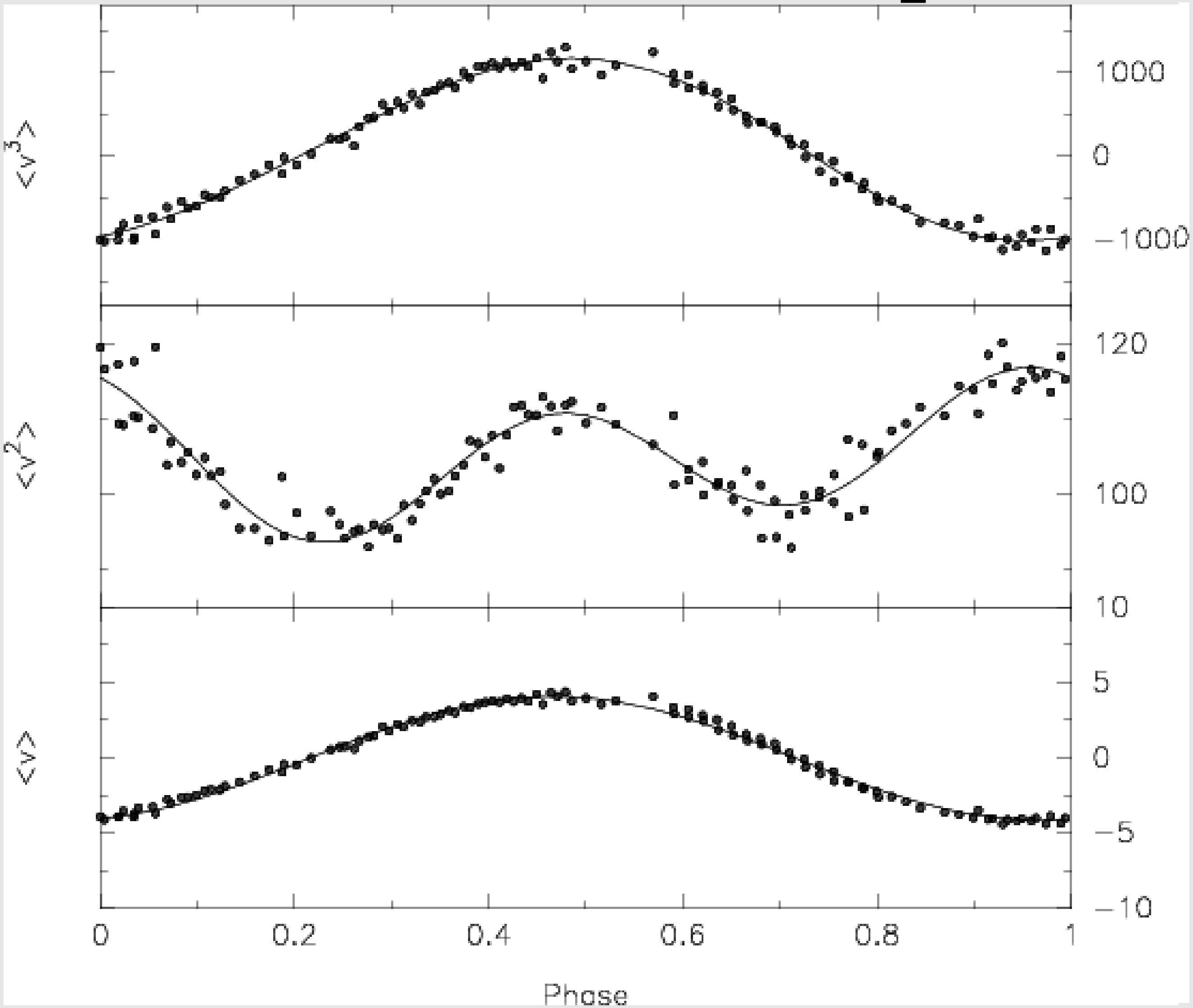

Rho Puppis has:

radial mode

amplitude ~ 5 km/s

vsini ~ 15 km/s

Applicability is limited to oscillations with amplitude > ½ EW

Outcome of a discriminant for Rho Pup

$$\gamma_l^m \equiv \min_{v_{\rm p}, i, v_\Omega, \sigma} \Gamma_l^m(v_{\rm p}, i, v_\Omega, \sigma)$$

l	$\|m\|$	γ_l^m	$v_{\rm p}$	i	v_Ω	σ
0	0	0.08	5.6	–	15.3	6.5
1	1	0.13	10.0	38°	14.8	5.9
2	1	0.17	12.1	64°	16.4	2.2
1	0	0.18	5.0	7°	19.6	1.7
2	2	0.23	15.0	53°	10.3	4.8
⋮	⋮	⋮	⋮	⋮	⋮	⋮

Don't forget to check the IACCs...

Multiperiodic moment method

Generalisation for multiperiodic pulsations with N frequencies shows :

- expressions for the moments are more complicated
- coupling terms appear due to the interaction of the different modes
  $\longrightarrow$ long observation runs are necessary
- the same discriminant can be used, but more computer time consuming
- use numerical version of moment method: Briquet & Aerts (2003)

Use moment method for identification in slow rotators and for stars with dominant mode

Phase changes across the profile

- Idea: map the stellar velocity field into the line profiles
- Pioneering study: bumps that pass through line are measure of m
- Application to fast rotators, as bumps need to be resolved
- That is problem.... NRP theory invalid... + restrictions to l=m, i=90°

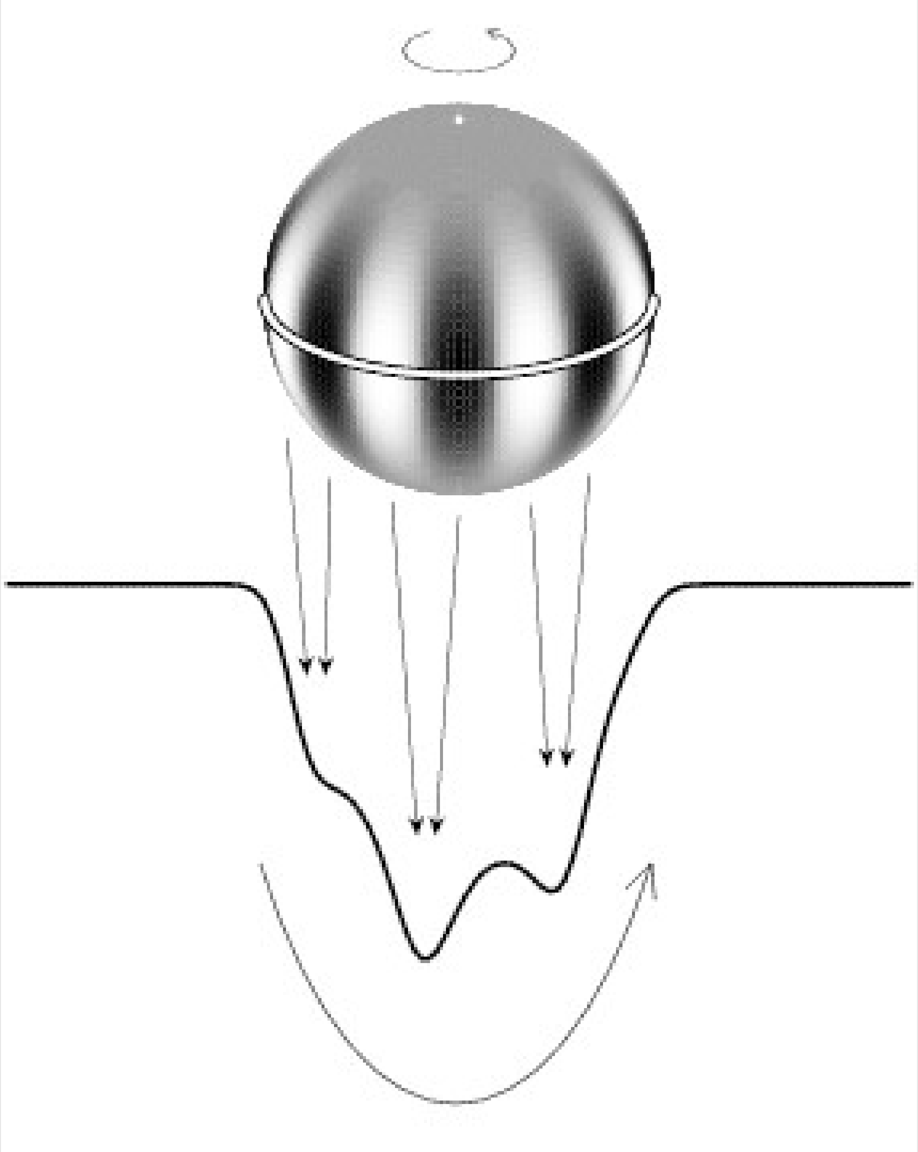

Simulations of LPVs

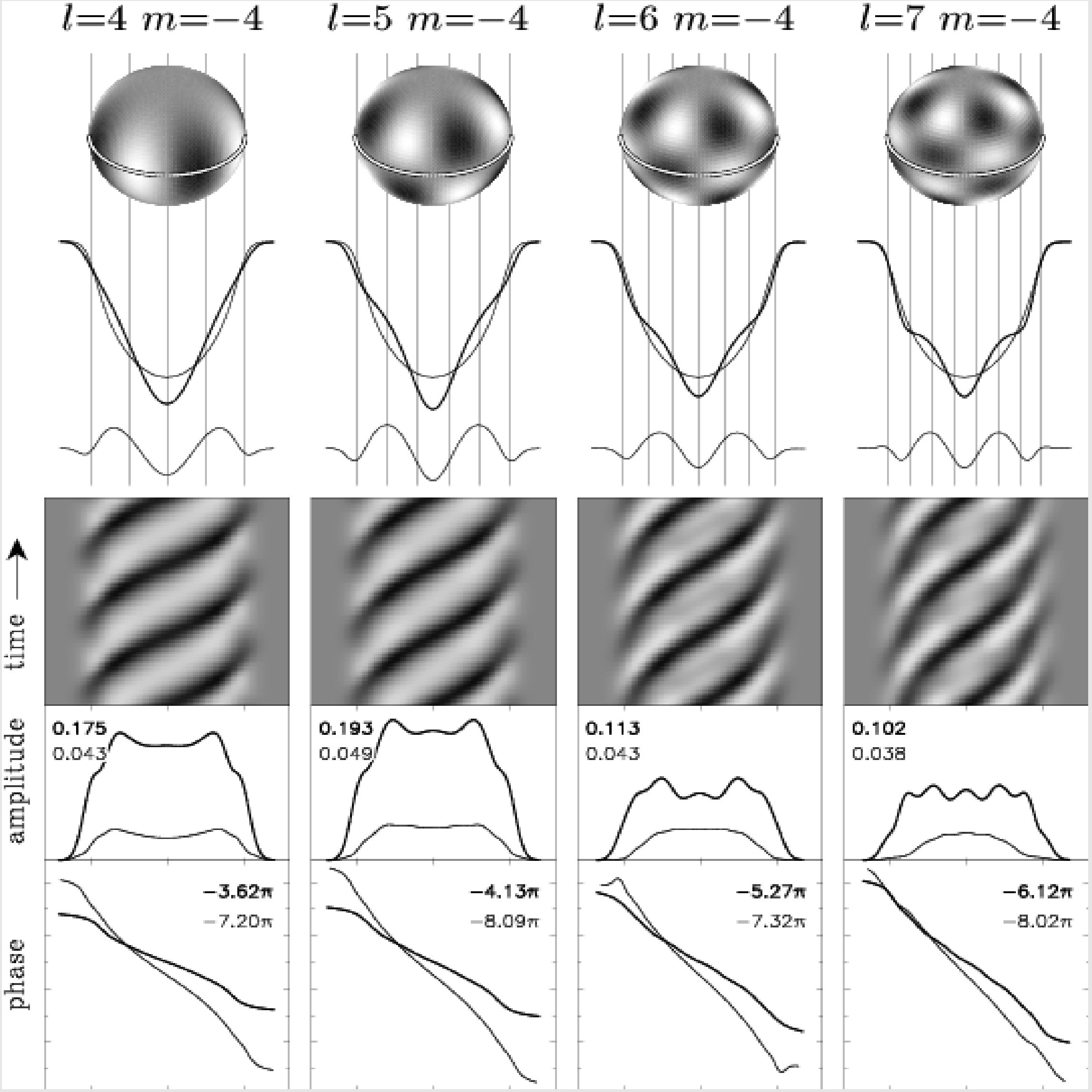

Telting & Schrijvers (1997) performed extensive simulation study for modes up to l=15

Phase change across the line profile

Doppler Imaging: original idea from Gies & Kullvanijaya (1988)

Telting & Schrijvers (1997) did much better job:

- LPVs based on code that includes Coriolis force
- extensive simulations: info is contained in harmonic as well
- number of phase changes is indicator of l
- number of phase changes of 1st harmonic may be indicator of m

A good estimate of l is: $l \approx (0.10 + 1.09\,|\Delta\psi_0|/\pi) \pm 1$

A good estimate of m is: $m \approx (-1.33 + 0.54\,|\Delta\psi_1|/\pi) \pm 2$

For concrete applications: do star-by-star analysis !

Application to Beta Cephei

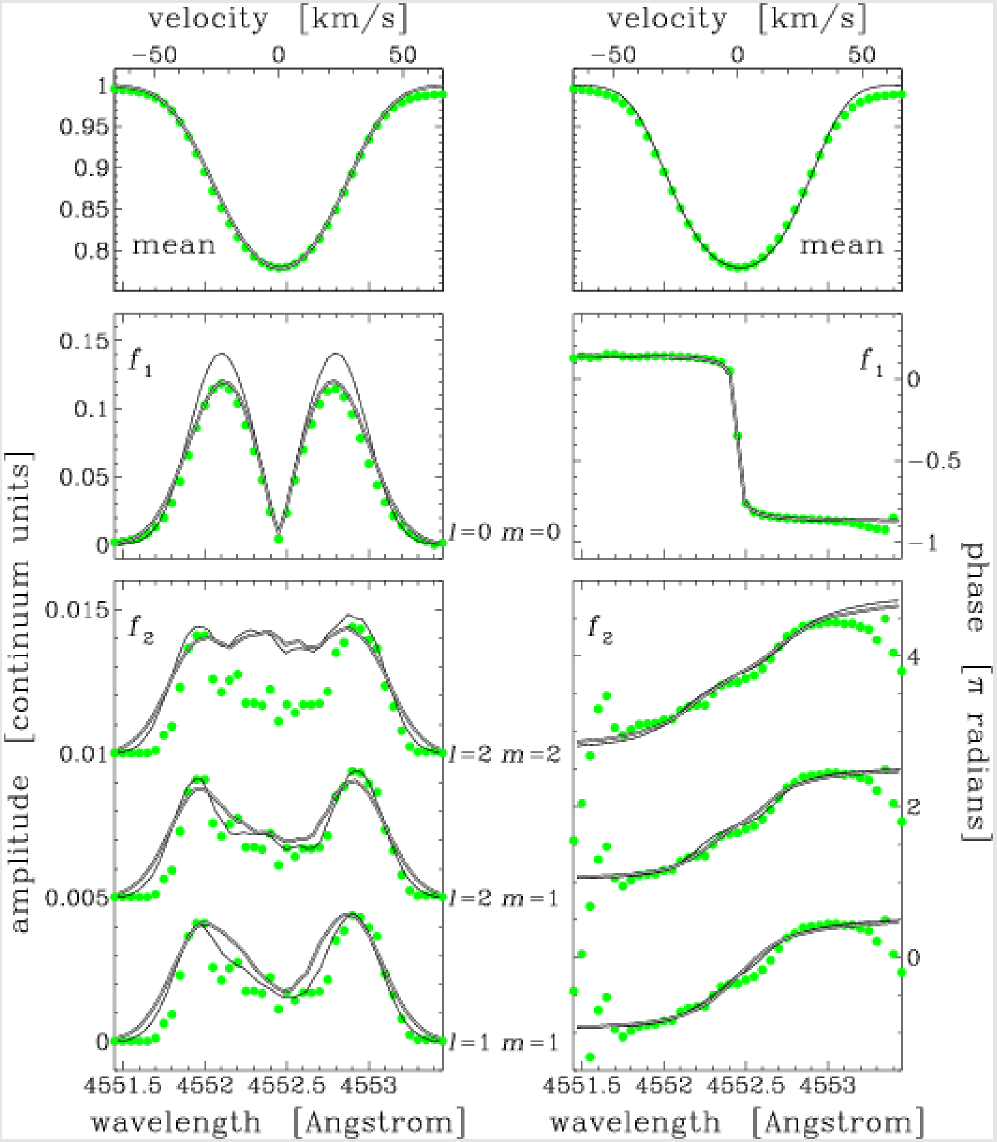

Beta Cephei has:

dominant radial mode with amplitude ~ 20 km/s

second low-amplitude mode: discrimination between l=1,2 is difficult but m=+1

Veq ~ 25 to 30 km/s

(Telting et al. 1997)

Pixel-by-pixel method: Zima (2006)

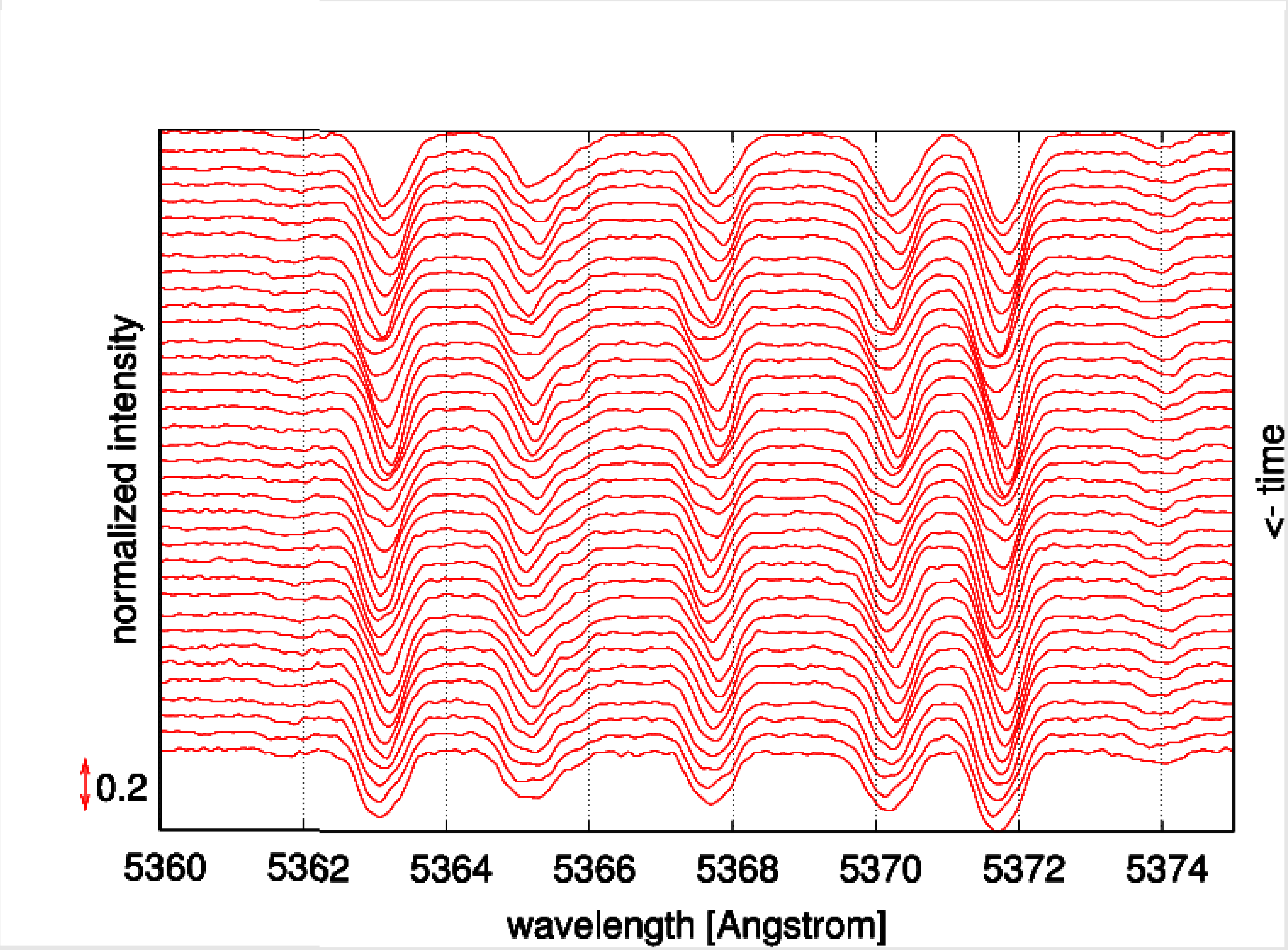

Estimate average line profile and work with residuals

Consider deviation parameter in Chi^2 sense and couple this to significance criterion

Application to FG Vir: Zima et al. (2006)

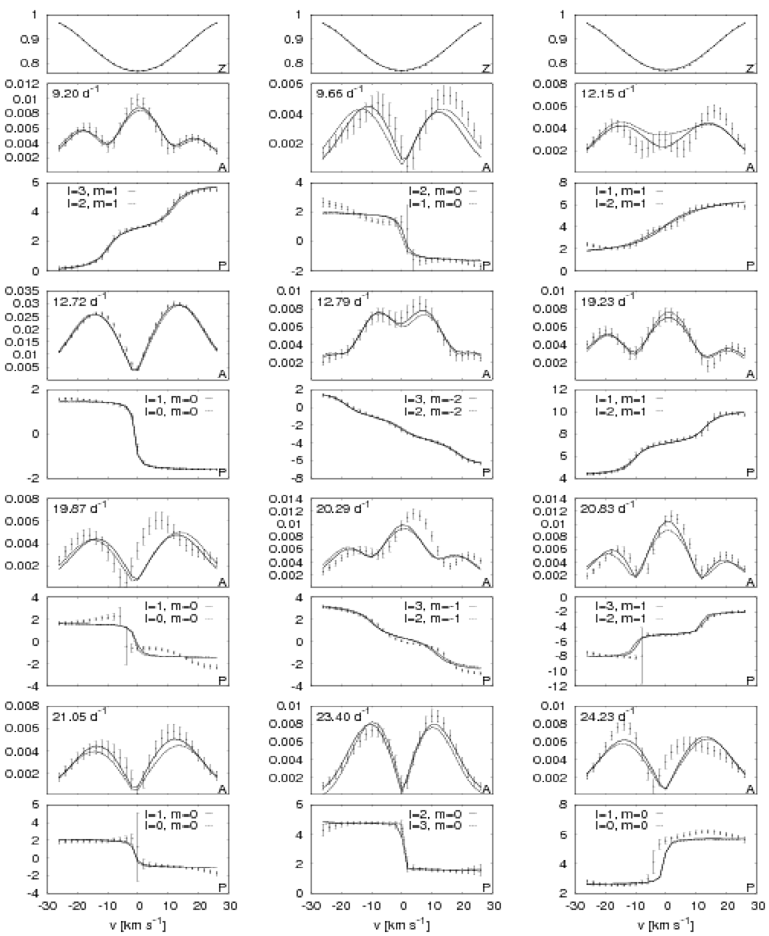

FG Vir has:

multiple modes (79!)

amplitudes ~ 2 km/s

Veq ~65 km/s

12 NRP could be identified from spectra:

6 have m ≠ 0

6 have m = 0

In agreement with photometric mode identificaiton

Conclusions (1)

- Sophisticated methods for interpretations of line-profile variations have been developed
- Frequency search can be done on moments or on pixel-by-pixel variations across the profile(s)
- Moment method is optimal for slow rotators; pixel-by-pixel method is better for faster rotators (BUT: not TOO fast to be compliant with theory)
- Moment method is not very sensitive to EW variations; pixel-by-pixel method is
- Moment method is not very sensitive to inaccurate average profile; pixel-by-pixel method is

Conclusions (2)

- Preferrably use both methods and compare results
- Methods discussed here can also be applied to
  - An average of several spectral lines, provided they are formed in same line-forming region
  - A Cross-Correlation function (CCF) derived from a full spectrum
  - A least-squared deconvolution (LSD) derived from a full spectrum

=> be careful for effects of line blending !!

(make sure it does not induce solutions close to an IACC...)

Conclusions (3)

- If both a time series in photometry and spectroscopy are available:
  - search for frequencies in both of them
  - use photometric mode identification for l and fix this in spectroscopic mode identification; compare results when l is not fixed
- Unambiguous identification of (l,m) helps a great deal to recognise merged multiplets...
- Even correct identification of (l,m) for ONE mode is significant step forward for seismic modelling

The package FAMIAS will help you to apply the moment method and the pixel-by-pixel method